Spatial risk assessment of silver fir and Norway spruce dieback driven by climate warming

Christian Piedallu (christian.piedallu@agroparistech.fr)
AgroParisTech - Centre de Nancy
Donatien Dallery
AgroParisTech - Centre de Nancy
Célia Bresson
AgroParisTech - Centre de Nancy
Myriam Legay
AgroParisTech - Centre de Nancy
Jean-Claude Gégout
AgroParisTech - Centre de Nancy
Rodolphe Pierrat
National Forests Office

Research Article

Keywords: climate change, forest dieback, decline, drought, tree vulnerability, vulnerability map

Posted Date: April 8th, 2022

DOI: https://doi.org/10.21203/rs.3.rs-1528617/v1

Abstract

Context: A significant forest decline has been noticed these last years in Europe. Managers need tools to better anticipate these massive events.

Objectives: We evaluated the efficiency of easily available data about environmental conditions and stand characteristics to determine stand vulnerability and map different levels of risk.

Methods: We combined remote sensing images, photo-interpretation, and digital models describing environmental conditions within a modelling approach to achieve spatial risk assessment of stand vulnerability. We focused on silver fir and Norway spruce stands in the Vosges mountains (8.800 km², north-east of France), where severe symptoms of decline are visible.

Results: Easily available factors describing environmental conditions were used to design relevant vulnerability maps: using an independent dataset, we predicted two-times (Norway spruce) and ten-times (silver fir) higher mortality rates in the units with a high level of risk compared to the others. Norway spruce were predicted highly vulnerable on 33% of their area *versus* 7% for silver fir. Mortality was higher where the soils displayed low water availability and had suffered severe drying events these last years; it was lower when the species belonged to uneven-aged stands, in mixture, and in the absence of forest edges. Furthermore, the stands acclimatised to drought conditions were more resilient.

Conclusions: Vulnerability maps based on easily available geographic information describing climate, soil, and topography can efficiently discriminate canopy mortality patterns over broad areas, and can be useful tools for managers to mitigate the effects of climate change on forests.

Introduction

With a global mean temperature increase of at least 1.1°C and changes in rainfall patterns, the effects of the ongoing climate change are more and more visible and consequential on ecosystem functioning (Pörtner et al. 2022). Increased tree mortality and changes in forest structure and composition have been observed in different biomes (Allen et al. 2015; Michel and Seidling 2018). In the western United States, van Mantgem et al. (2009) demonstrated a doubling of the rate of background tree mortality every 17 to 29 years, while Peng et al. (2011) observed a 4.9% increase in tree mortality per year from 1963 to 2008 in Canadian boreal forests. In Europe, remote sensing data have revealed a 2.4% increase of canopy mortality *per* year between 1984 and 2016 (Senf et al. 2018), and different hotspots have been identified in the north or the south of the continent (Neumann et al. 2017). These trends were most of the time attributed to the recent changes in climate (Han and Singh 2020; Senf et al. 2020). An excess of tree mortality has been associated to the current changes in temperature or rainfall for about half of the most common European tree species (Taccoen et al. 2019). The impact of climate change on forest decline is expected to persist in the future: climate projections predict that warming will continue, involving decreased water availability for plants and more extreme weather events (Pörtner et al. 2022).

Climate-related forest dieback is of particular concern because of the huge economic stakes and the essential ecosystem services provided by forests, including carbon storage, water protection, erosion control, or habitat provisioning services (Brockerhoff et al. 2017). Forest dieback also has an effect on local or regional climate conditions by increasing the albedo and heat fluxes (Anderson et al. 2011). Despite the major importance of the issue, the way forests will cope with climate change remains highly uncertain. Vulnerability assessments are done *a posteriori* most of the time, and forest managers cannot anticipate massive mortality events. The choice of the tree species – traditionally based on specific ecological requirements – can no longer correspond to current climate conditions (Torssonen et al. 2015). In a context of increasing impacts of recent droughts on ecosystems in a large part of Europe (Buras et al. 2020), evaluating the mortality risk across broad areas is crucial to mitigate the effects of climate change.

The death risk is a natural component of the forest dynamics that can be increased by different stresses. Tree decline is often described as a gradual process involving different causes and cumulative effects. It has been presented as the combination of interchangeable predisposing, inciting, and contributing factors (Sinclair (1965). Predisposing factors reduce tree ability to resist to a stress on the long term, inciting factors are usually caused by extreme events (Maringer et al. 2021) and contributing factors are often insects or pathogens that cause the final decline through hydraulic failure or carbon starvation (McDowell et al. 2008). This model based on different causes that interact at different time and spatial scales was popularized by the decline spiral in the 1980's (Manion 1981).

Predisposing factors are mainly related to tree or stand characteristics, poor site conditions or air pollution. Age and tree competition for light are important drivers of tree mortality. Tree growth leads to overcrowding and natural mortality through self-thinning, particularly for suppressed trees or high-density stands (Charru et al. 2012). Mortality is also influenced by species interactions, stand structure or silvicultural practices (Taccoen et al. 2019). In addition, trees are more threatened when temperature is high or water availability is low (Brandl et al. 2020). An effect of the soil nutritional properties has also been demonstrated (Maringer et al. 2021). Finally, air pollution due to nitrogen, sulphur deposition and ozone can also contribute to the weakening of forest ecosystems (Dietze and Moorcroft 2011). Atmospheric deposition increases aluminium concentrations in the soil, and toxic levels can be reached.

Inciting factors are mainly drought events, heat waves, frost, snow, forest fires, floods, or storms. Allen et al. (2010) identified more than 150 references of forest mortality driven by extreme events since 1970. The deleterious effects of droughts and heat waves on tree fitness have been studied extensively (Choat et al. 2012; Urli et al. 2013; Williams et al. 2013). These events can trigger severe dieback (Buras et al. 2020; Senf et al. 2020), sometimes with delayed effects (Lebourgeois 2007). In the current climate change context, their frequency and their intensity have increased since the beginning of the 21st century (Hartmann et al. 2018). Storms also play an important role by weakening trees and promoting biotic outbreaks (Marini et al. 2017). Their impact is expected to increase due to the increasing growing stock combined to the effects of changing climate (Schelhaas et al. 2003).

Contributing factors are most of the time biotic agents: pests and diseases often lead to the death of the trees that have already suffered from predisposing or inciting factors. They can attack trees over important areas, and they are expected to be favoured by climate warming (Ward and Masters 2007). Several recent outbreaks of bark beetles are presented as among the most severe outbreaks ever seen (Lundquist 2019). At the end of April 2019, the French National Forest Office (ONF) estimated that 50% of spruce were affected by bark beetle attacks, *versus* 15% in the usual course of events (Office National des Forêts 2020 [1]).

The level of risk varies according to the species sensitivity (its capacity to resist to changing climate), local exposure (related to the intensity of the effects of climate change), and the adaptive capacity of the species (its ability to cope with the new climate conditions) (McCarthy et al. 2001). Different approaches have been implemented for managers to mitigate the effects of climate change on forest species, e.g., recommendations by expert knowledge according to site type maps, or more sophisticated risk assessment based on large databases from forest inventories or remote sensing data, coupled with mechanistic or statistical models. One of the most popular approaches is based on empirical niche models or process-based models (Coops and Waring 2011; Fremout et al. 2020). It simulates the suitable areas of the species according to contemporary or simulated climate. These models can be used to evaluate if the species can maintain itself under warmer climate conditions, or to track their current climate niche (Aubin et al. 2018). They have important limitations because the numerous assumptions often lead to overestimating the risk (Das et al. 2022). Vulnerability can also be estimated by modelling the level of dieback using the different factors that can alter tree fitness (Archambeau et al. 2019; Lu et al. 2019). Using this approach for spatial risk assessment over broad areas remains uncertain. Although many predisposing factors are often easily available, inciting or contributing factors are scarcely available, so that predictive performances may be poor.

Here we evaluated if easily available geographic information describing climate variability and evolution, and the main soil and topographic characteristics, can be combined with remote sensing images to efficiently discriminate landscape-level canopy mortality patterns at a regional scale. Focusing on two emblematic stand types of European mountain ranges – silver fir and Norway spruce – we modelled the tree health status collected from sentinel-2 data in 2019. We used variables describing the site conditions available from Geographic Information System (GIS) layers and the stand characteristics extracted from aerial photographs to identify the conditions that promoted decline. Based on these models, a vulnerability map was calculated at 50 m resolution in an 8,800 km² area, and evaluated with ground survey data providing the volumes of dead wood harvested from exceptional sanitary cuts.

[1] https://www.onf.fr/+/4bd::ces-arbres-forestiers-qui-souffrent-de-la-secheresse.html

Materials And Methods

Study area

The Vosges mountain range is located in the north-east of France (area: 8,800 km²). It has contrasting soil and climate conditions. Altitude ranges between 200 m in the eastern plains of Alsace to 1,424 m (Fig. 1A). Rainfall varies between 500 and 2,000 mm, and mean annual temperatures between 6°C and 11°C for the 1981-2010 period (Aurelhy model, Météo France). Geology mainly consists of acidic sandstones in the north and west of the study area, and magmatic rocks in the centre of the mountain range (Fig. 1B). Forests cover more than 60% of the territory, and provide important economic and social benefits[2]. The region experienced important tree decline events during the 1916-1925, 1943-1951, or 1973-1981 periods. During this last period, combined climatic stress after the 1976 drought and air pollution that increased nutritional difficulties led to magnesium deficiencies (Landmann et al. 1987). Silver fir and Norway spruce have gradually been declining since 2016, questioning managers and policy makers about the future of these species in the Vosges massif.

Mapping of dieback using remote sensing data

We used three Sentinel-2 images level N2A downloaded from Theia website[1]. We selected images taken on July 24, 2019, during a period with little cloudiness and maximum vegetation cover to avoid confusion between the soil and dieback, and differentiate dead trees from living trees. These images were corrected for atmospheric, topographic and geometric effects. Dieback was identified through a supervised classification by excluding bare soil, crops, ground vegetation, urban areas, water, and forested areas. The classification was trained using 288 units presenting dieback, and validated with 1,814 others units including 285 units presenting dieback, collected by photo-interpretation. The Sentinel-2 images were classified with ArcGIS Pro 2.5.0, using maximum likelihood classification (MLC, Sun et al. (2013)).

Sampling strategy

To avoid considering mortality patterns from other species than silver fir and Norway spruce, we used the IGN BD forêt v2[1] database to select vegetation units recorded on aerial photographs that showed these two species. A systematic 100-m grid was built, and 1,000 plots were randomly selected in dieback-struck areas and another 1,000 plots in healthy places.

We used aerial photos at 20 cm resolution to separate plots according to the dominant species (spruce or fir) and to identify the stand composition on 15-m-radius plots (seven classes, Online resource 1). We used photos dating back to 2018, taken prior to the dieback event, to identify the stand characteristics. To avoid the risk of confusion, only the classes where the studied species was dominant or not in mixture with the other studied species were kept for each dataset to avoid confusion (classes 1, 2, 3 and 5 in Online resource 1; 872 plots were selected for silver fir, and 1,043 plots for Norway spruce). For each plot, the stand's status (healthy or dieback) and 112 explanatory variables were collected in a database: 6 variables described the stand characteristics, 50 described the site conditions, and 56 described climate evolution.

Variables describing the stand characteristics

We distinguished four levels of species mixture (COMP, modalities 1, 2, 3 and 5, Online resource 1) within the stand characteristics variables (Table 1). DENS differentiated dense stands from sparsely forested stands, where the ground was visible on more than 10% of the plot area. To describe the age and structure effects, STRUCT was recorded in three classes: old even-aged forest stand, young even-aged forest stand, and heterogenous structure. TYP_EDGE identified the presence of edges due to interfaces between different land uses (absence of an edge, edge between 2 forest stands of different heights, and with an open environment), and EDGE_S identified edges facing south. These variables were collected using aerial photographs, on 15-m-radius plots (similar to classical forest inventory plots in France), for COMP, DENS, and STRUCT, and on 50-m-radius plots for TYP_EDGE and EDGE_S to consider data around the plot that could influence the stand health. Finally, we added data about the 1999 windstorm damage that had a strong impact on the Vosges mountains forests by rejuvenating some forest stands. IGN maps differentiated areas with less than 10% damage from those with 10 to 50% damage or more than 50% damage.

Variables describing the site conditions

Fifty variables described the site conditions. They concerned geology (n=1), topography (n=9), soil nutrition (n=2), waterlogging (n=2), energy for plants (n=12) and water availability (n=24) (table 2). A simplified geological map (GEOL) was drawn by merging similar substrates on the local maps at 1:50,000 scale elaborated by the BRGM. Topographical indices were calculated with the IGN 50-m DEM for altitude (ALT), aspect – cosine of aspect (COS_ASP), sine of aspect (SIN_ASP) –, and slope (SLO). Topographical position was represented by four indices: containment (CONT), the difference of altitude between the pixel and the average altitude within a 1,500-m radius, curvature (CURV) that describes the shape of the topographical surface in the direction of the maximum slope within a 1,500-m radius (convex, flat or concave), TOPO and REL_ALT that are the relative distance and altitude of the cell along the toposequence (the ratio of the distance or altitude between the cell and the nearest ridge to the total length or the difference of altitude found in the toposequence), respectively. We characterised soil nutrition and waterlogging according to 1-km resolution maps built using bioindication techniques (Gegout et al. 1998) for soil surface pH, nitrogen nutrition (C/N ratio, CN), temporary waterlogging (TW) and permanent waterlogging (PW).

GIS layers of monthly climate variables were used to estimate energy and water available for plants over the 2009-2019 period. Solar radiation (RAD) was calculated at 50 m resolution using Helios model (Piedallu and Gegout 2007). Monthly minimum, average and maximum temperatures and rainfall (TMIN, TMEAN, TMAX, and RAIN, respectively), were modelled and mapped at 1 km resolution (Piedallu et al. 2016). Climatic water balance (CWB) is the difference between RAIN and potential evapotranspiration according to Turc's formula (Turc 1961). One-km resolution maps of soil depth (DEPTH) and soil water holding capacity (SWHC) (Piedallu et al. 2011) were used to evaluate the soil water content (SWC, available water in the soil) and the soil water deficit (SWD, the difference between potential evapotranspiration and actual evapotranspiration) according to Thornthwaite formula (Thornthwaite and Mather 1955). In addition, three indices characterising lateral fluxes in the soil were extracted from GIS

layers. Kh and Kv represented the horizontal and vertical hydraulic conductivity at soil saturation, respectively, and FLUX estimated the balance between the input and output surface and subsurface fluxes (Ondo et al. 2017).

All the variables including climate were averaged over the ten years before data collection (2009-1019), *per* season (winter -wi, December to February-; spring -sp, March to May-; summer -su, June to August; and autumn -au, September to November), and over the whole year (an).

Variables describing climate evolution

Two sets of calculations – climate anomalies and climate trends – were used for TMIN, TMEAN, TMAX, RAIN, CWB, SWC and SWD. Climate anomalies represented the evolution between a reference period and a contemporary period. A period of ten years before data collection (2009-2019) was selected to represent the contemporary period because tree death can be triggered by the cumulative effects of many disturbances (Das et al. 2013). We selected 1961-1985 as the reference period because significant warming occurred in France after 1986 (Taccoen et al. 2019).

Climate trends were calculated for the same variables over the 1986-2019 period. For each variable and each pixel of 1-km resolution, the trends were regressed against time for the 32 studied years, and the linear regression coefficients were mapped. A positive slope indicated an increase of the climatic constraint for TMIN, TMEAN, TMAX and SWD, and a decrease for RAIN, CWB and SWC.

Modelling approach and vulnerability map calculation

We modelled silver fir and Norway spruce mortality with logistic regression (McCullagh and Nelder 1997). For each species, we evaluated the 113 explanatory variables through a forward stepwise procedure. At each step, the variable explaining the maximum deviance was selected if it was statistically significant ($P < 0.01$), and little correlated with the previously selected variables (Pearson's $r < 0.7$). Because monotonic responses were expected, quadratic responses were not considered for the climate variables. However, monotonic and quadratic response curves were both evaluated for the other variables. The process ended when the selection of a new variable led to a d^2 increase lower than 0.01 or a p-value > 0.01.

The receiver operating characteristic (ROC) curve was calculated to evaluate the performances (Fielding and Bell 1997), and different metrics were used: the area under the ROC curve (AUC), the kappa index, success (the rate of good prediction), sensitivity (the rate of good prediction of presence), and specificity (the rate of good prediction of absence) (Manel et al. 2001). The relative importance was calculated for each variable using the drop contribution (Lehmann et al. 2002), *i.e.,* the difference in explained deviance between the full model and a partial model when the variable was dropped. The ratio of the drop contribution of the variable over the sum of the drop contributions for all the variables gave the relative importance of each predictor.

The ROC curve also provided the optimal threshold for predicting the presence / absence of dieback. It was used to calculate the vulnerability map: upper values delineated the "high level of risk" class where

the stands were predicted dead by the model, while lower values were divided in three classes with equal intervals of increasing risk. The vulnerability map was calculated using the GIS layers describing the environmental predictors selected in the model. It included four levels of risk, calculated from a type stand used across the whole area.

Validation dataset

A map of the volumes of harvested dead wood from exceptional sanitary cuts was provided by the ONF for public forests, which cover 2/3 of the forested area of the Vosges mountains. We selected areas where one of the studied species was dominant or not in mixture with the other studied species. For 7,355 management units identified for silver fir (11,218 for Norway spruce), the average volume of dead wood was compared for the different vulnerability levels. Our vulnerability maps were drawn using 2019 satellite imagery, but dieback may have occurred before or after this date in the most vulnerable areas. As a consequence, we considered both the volumes of dead trees recorded in 2019 and the sum of the volumes over the 2018-2020 period.

[2] https://theia.cnes.fr/atdistrib/rocket/#/search?collection=SENTINEL2

[3] https://inventaire-forestier.ign.fr/spip.php?article646

Results

Distribution of silver fir and Norway spruce dieback in the Vosges mountains

The classification of sentinel-2 data predicted 92% of the stand status of the validation dataset correctly. It identified 2,072 ha of dieback in the Vosges mountains, representing 1.4% of the studied stands. We observed dieback on 362 plots out of the 872 plots selected for silver fir, and on 627 plots out of the 1,043 plots selected for Norway spruce, mainly in the south and the north of the studied area (Fig. 2). Eighty-five plots were deleted due to the risk of confusion because the two species were in mixture and neither was dominant, or the stands were too young and the species were impossible to identify.

Silver fir and Norway spruce dieback modelling

With respective AUCs of 0.80 and 0.78 and nine variables selected, the silver fir and Norway spruce dieback models showed similar performances and near predictors (Figs. 3 and 4). They combined variables describing stand composition and structure, local conditions and climate evolution to various extents according to the species (Online resource 2). Environmental conditions explained 59% of the deviance for silver fir *versus* 62% for Norway spruce. Geology and stand composition were among the most important variables correlated with dieback for both species, in addition to the presence of an edge southward for silver fir and temporary waterlogging for Norway spruce. The trend in summer soil water deficit was directly linked to climate change (relative importance ranging between 6 and 7%).

Less dieback occurred for both species when they were in mixture in stands dominated by broadleaved species. Mortality was significantly higher in pure stands for Norway spruce (Figs. 3 and 4). More dieback was also identified in even-aged stands compared to uneven-aged or young stands when a forest edge was present (with a clear effect of a south forest edge for silver fir), and in stands that underwent little damage during the 1999 storm. Silver fir and Norway spruce mortality also responded to five environmental variables (Figs. 3 and 4). Silver fir showed a higher risk of dieback when it grew on volcanic pyroclastic rocks, neutral to basic rocks, principal conglomerate or acidic granite. Norway spruce showed lower substratum-dependent differences than silver fir did, and was more prone to dieback on sedimentary basic rocks, Voltzia or shell sandstone. Both species were also sensitive to topographical position, with a higher risk of dieback in areas near the ridges, on the south slopes, and when waterlogging was present. Finally, increased dieback was observed with soil drying. High values corresponded to a strong increase of the soil water deficit during the 1986–2019 period (Figs. 3 and 4, equations for the two species can be found in online resources 3 and 4).

The risk of dieback linked to environmental conditions and stand characteristics varied according to the location for both species (Fig. 5, 6, B, C). The vulnerability maps calculated at 50 m resolution (Fig. 5-D and 6-D) identified 7% of the stands with a high level of risk for silver fir *versus* 33% for Norway spruce, while 83% of the stands were classified as presenting a low or very low level of risk for silver fir *versus* 26% for Norway spruce (Fig. 7). In the validation dataset (Fig. 8), we observed a significantly higher volume of dead trees for the class showing a high level of risk than for the other classes. This difference was higher for silver fir (about ten-fold) than for Norway spruce (about two-fold).

Discussion

Large surfaces of silver fir and Norway spruce stands are threatened in the Vosges mountains

Tree species vulnerability is an issue of growing concern round the world, but it is not new in managed forests. After the 1911 drought in the centre and west of France, Roulleau already reported, “I see everywhere […], in the cooler parts like the drier ones, a lot of trees are dying […] I have long recommended caution in the use of Norway spruce” (Roulleau 1912). These observations concerned lowland areas, where the species was introduced outside of its natural range. Conditions are different in the Vosges mountains, that benefit from colder and wetter conditions typical of middle mountains of European climate. In this area, silver fir is a native, emblematic species, while Norway spruce is considered as natural near the top of the mountain range (Guinier 1959). Yet, we found large surfaces threatened by forest decline. In agreement with other studies (Maringer et al. 2021), we observed a higher vulnerability of Norway spruce than of silver fir.

We probably under-estimated the surfaces concerned by dieback because isolated dead trees or low symptoms were probably not identified by remote sensing approaches, and the dead trees in some of the dead stands were probably felled by forest managers before the satellite images were taken. This

probably decreased the model performances, but with a limited influence on the estimation of vulnerable areas, as cuts concern a wide variety of ecological and stand conditions. We chose a spatial approach aimed at linking the spatial heterogeneity related to site conditions and stand characteristics with the regional patterns of dieback. This approach should be complemented by a temporal follow-up of the dieback dynamic using time series images and requiring inventories at different periods, to better identify recent cuts of dead trees and simulate probabilities of dieback according to future climate conditions (Knight et al. 2013; Staupendahl and Zucchini 2011).

A relevant method for large-scale spatial risk assessment

The levels of risk estimated on the vulnerability map successfully discriminated the volumes of dead trees recorded in public forests, highlighting the benefit of using easily available geographic information for the spatial risk assessment of silver fir and Norway spruce dieback. Despite less precision compared to traditional ground surveys, the use of satellite imagery, photointerpretation and digital maps of environmental factors allowed us to sample a large number of plots distributed along large environmental gradients. As far as the mapping results are concerned, the better performance of silver fir compared to Norway spruce can be explained by the large extent of Norway spruce dieback across a wide variety of ecological conditions, and its higher susceptibility to bark beetle attacks (de Groot and Ogris 2019). The resolution of the GIS layers describing the spatial variations of the environmental predictors probably influenced the performance of the vulnerability map (Cavazzi et al. 2013). The selected variables were at 50 m resolution for relative altitude and the cosine of aspect, at 1:50,000 map scale for geology, and at 1 km resolution for temporary waterlogging and the trend in soil water deficit. Because dieback can vary at a very local scale, finer resolution predictors could improve the vulnerability map.

Existing risk assessment was mostly based on mortality observed the previous years (Preisler et al. 2017), changes in tree fitness visible by satellite imagery (Verbesselt et al. 2009), or the identification of weakened trees with declining growth (Suarez et al. 2004). We propose a method based on easily available geographic information, that can be implemented over broad areas, to monitor dieback of different species and over different periods of time. When data is available, it can be coupled with forest inventory information for a better description of the stand characteristics. The risk of decline was predicted efficiently, although inciting and contributing factors were not explicitly considered. We expect that they were indirectly and partly taken into account by the climate variables selected in the models. The trend of the soil water deficit variable is probably influenced by the extreme drought events and linked to the distribution of pathogens, which is also linked to climate variables (Baier et al. 2007). This result was probably observed because bark beetle attacks – which are severe in the area – occur preferentially on weakened trees (Kolb et al. 2019). The model performance could probably be improved by including variables concerning extreme events and disturbances when available: for example, wind conditions and storm frequency, drought intensity, forest fires (Carnicer et al. 2011), air pollution (Pedersen 1998), or biotic attacks (Jaime et al. 2019).

According to the classification of sentinel-2 images, observed dieback at a specific date is a relatively rare statistical event. To overcome this limitation, the proportion of areas with dieback was oversampled by

selecting 50% of plots in dieback areas to calibrate the models. This method yielded correct regression coefficients, but it increased the intercept value. Consequently, the probability of dieback in the model outputs was overestimated (King and Zeng 2001). Therefore, the probability of dieback provided by our modelling should not be interpreted as real probabilities, but it makes it possible to compare the effects of the qualitative variables and to interpret the shape of the response curve for the quantitative ones. This oversampling effect was corrected for the vulnerability map by using the ROC curve, that determined the classes of increasing levels of risk according to the optimal statistical threshold for each species.

Dieback is explained by a combination of site conditions and stand characteristics

The selected variables were linked to stand characteristics, geology, and water availability, with a clear effect of climate change. Large differences were highlighted relatively to the latest important tree decline event experienced in Europe during the 1973–1981 period. At that time, climate stress after the 1976 drought and air pollution that increased the nutritional stress and led to magnesium deficiencies were identified as the main factors that triggering forest decline (Elling et al. 2009; Landmann et al. 1987; Vitali et al. 2017). In 1984, 26% of silver fir and 17% of Norway spruce lost more 20% of their needles according to an observatory network encompassing the Vosges mountains. More mortality was observed for old trees located at low or high altitudes, on acidic substratum, and in the east of the mountain range (Bonneau 1985; Thomas et al. 2002). We are now observing lower mortality at high altitude, no more mortality on acidic substratum compared to the other areas, and a greater decline in the south and the north of the mountain range. These differences suggest that dieback is currently triggered by different factors than those identified during the 1980's.

Importance of water availability in silver fir and Norway spruce dieback

Dieback of both silver fir and Norway spruce responded markedly to water balance variables in our models. The soil water deficit trends performed better than climate anomalies or variables describing average climate. This result stresses the importance of the dynamic of soil water availability in dieback evaluation. The effects of drought on tree decline have been largely studied, but most of the large-scale studies tried to relate forest dieback to average climate conditions over long periods (Lu et al. 2019). For a given current soil water deficit, we observed that impacts on trees were greater when the deficit had sharply increased in the last years compared to areas under recurring deficit (Online resource 5). These outcomes suggest that a tree of a given species can be more resilient to drought when it has grown in drier conditions, as observed by Gazol (2017) both in the north of America and Europe. They also highlight that the dynamic of water stress over time should be considered rather than average climate to forecast mortality patterns. Our understanding of the time span that should be investigated to efficiently evaluate stand vulnerability should also be improved.

Several other selected variables were related to water availability. The higher risk of dieback observed near the ridges was related to the lateral redistribution of the soil moisture along a topographical hillslope

gradient (Ondo et al. 2017). Some authors reported 15 to 90% lower soil moisture near the crests compared to the valleys (Western et al. 2004). The more severe dieback symptoms on south slopes can be attributed to their higher evaporation and transpiration, and differences in thawing. Rouse et al. (Rouse and Wilson 1969) observed 50% more water stored in the north slope soils than in the south slope soils in early spring. The increasing mortality with temporary waterlogging intensity can be interpreted in different manners. Both silver fir and Norway spruce avoid compact or waterlogged soils. Waterlogging also influences the plant water uptake by affecting the spatial distribution of fine root growth and limiting their depth (Fujita et al. 2021). Finally, the presence of edges (particularly south edges for silver fir), stresses the importance of microclimatic conditions. Increased temperature, light, and wind speed that increased evapotranspiration and decreased the soil water content have been recorded from 40–50 m from the edge (Chen et al. 1995), leading to higher tree mortality rates (Mesquita et al. 1999). These predictors related to the water balance represented 51% and 48% of the explained model deviance for silver fir and Norway spruce, respectively. They all showed an increase of dieback when the water balance components shifted toward less available water for trees.

Stand characteristics complement environmental predictors to explain dieback

Although stand data were collected by photo-interpretation – a less accurate method than field inventories – we demonstrated that stand characteristics could also explain dieback, with similar responses of the two studied species. We observed less mortality for uneven-aged stands and mixtures. These results are in agreement with previous studies showing lower resistance to disease and damage in even-aged stands than in uneven-aged stands (Pukkala et al. 2013). The negative effect of pure stands supports the results of previous studies demonstrating the benefits of functional diversity on tree resilience (Gazol and Camarero 2016), which can be explained by facilitation and resource partitioning. Facilitation is an interaction between species that benefits to at least one of them, while resource partitioning refers to the way different species can share resources over time or across space (Mc Cook 1994). Lower Norway spruce dieback was shown in stands dominated by beech (Pretzsch et al. 2020), attributed to complementarity in water uptake. A temporal shift between the two species provided Norway spruce better resistance to drought events (Rotzer et al. 2017). These effects are greater in low-productivity sites, as already observed in the Vosges mountains (Lebourgeois et al. 2013).

We also found less dieback in young stands or stands that had suffered important damage during the 1999 storm. The lower mortality of small trees compared to large ones could be attributed to differences in fine root distribution, in vulnerability to biotic factors, and to the greater water uptake difficulties of tall, large trees (Pfeifer et al. 2011). Because silver fir and Norway spruce dieback increase with basal area (Taccoen et al. 2019), this lower mortality could also be linked to limited competition for light or water in young stands. Lowering the basal area is often considered as a silvicultural tool to decrease tree vulnerability to drought and improve productivity (Pretzsch 2005). In agreement with studies demonstrating the strongest negative growth trends in pure and even-aged productive forests of conifers (Ols and Bontemps 2021), we suggest to promote an evolution of silvicultural practices toward mixed

stands of uneven-aged trees to limit the stand basal area and avoid brutal cuts to limit edge effects (that can also reduce wind damage). The cumulated effect of these measures would lead to a significant decrease of the dieback risk for the two studied species.

Using the map to mitigate the effects of climate change on silver fir and Norway spruce forests

The vulnerability map makes it possible to prioritise the level of risk for each studied species in view of helping forest managers to mitigate the effects of climate change. The map can be used directly because it instantly provides an evaluation of the risk based on environmental conditions according to the geographic location. When basic information about stand structure and composition can be surveyed (using ground surveys or aerial photographs), the prediction can be improved: the effects of the stand characteristics can be evaluated, and the map gives information about the potential decreasing risk if the stand characteristics allow for better tree resilience.

The future of Norway spruce and silver fir is probably strongly compromised in the most vulnerable areas identified by a high level of risk on the map. These two species should be monitored in these areas on a priority basis, e.g., by raising the rate of transparency of the crown in some representative plots, or by using NDVI indices based on remote sensing data (Rogers Brendan et al. 2018). They should be preferentially cut when the first signs of degradation appear, and should not be replanted afterwards. Reforestation should rely on adequate forest regeneration promoting drought-tolerant species if available. Species more resistant to drought could also be introduced by selecting species that are visually close to those they replace in areas of high landscape interest. When the level of risk is low or moderate, the strategy can be to promote a rapid evolution of silvicultural practices to adapt stand structure and composition in priority. The aim is to mitigate the effects of climate change in areas that can become highly vulnerable in the next decades. The areas with the lowest level of risk would not be a priority in the first place but should also be monitored. The vulnerability map should be updated at regular time intervals to take the evolution of the soil water deficit and observed mortality changes into account, and adjust recommendations accordingly.

Conclusion

Our results demonstrate an important impact of recent climate change that increased forest dieback by limiting water availability in Norway spruce stands, and also in silver fir stands to a lesser extent. Vulnerability maps can help to adapt forests to current new climate conditions. Harvesting trees following dieback events causes a financial loss, is a logistical challenge, contributes to pathogen infestation, and creates an important opening up of the environment that modifies microclimates, impairs future reforestation and impacts ecosystem services. The massive disappearance of trees could also have important impacts on biodiversity and ecosystem services by increasing the risk of natural hazards, preventing the preservation of water resources, and altering landscape quality on the long term. We calculated a vulnerability map for the current period; its extrapolation to future conditions remains questionable. The risk of decline will probably be influenced by the evolution of water availability in the

next years, and the maps should be updated at regular intervals. In the short term, a potential succession of wet summers might limit dieback. In the long term, increasing temperatures and drought leave little hope for the future of Norway spruce in a large part of the Vosges mountains, where its decline is already widespread. The situation is more contrasted for silver fir, and the evolution of water availability in the coming years will influence its evolution. We can reasonably expect stands with a low level of risk to be spared in the next decades.

Statements & Declarations

Fundings

The Unité Mixte de Recherche (UMR) SILVA is supported by a grant overseen by the French National Research Agency (ANR) as part of the 'Investissements d'Avenir' program (ANR-11-LABX-0002-01, Lab of Excellence ARBRE).

Competing Interests

The authors declare no conflict of interest or competing interests.

Author's contribution

D.D. performed the remote sensing analysis, C.B. contributed to the GIS analysis, I.S. and J.C.G. provided bioindicated indices, R.P. provided data from exceptional sanitary cuts, M.L. and C.P. developed the study conception and design, C.P. performed the data collection, realized the analysis and wrote the paper. All of the authors read and corrected the paper, and gave their final approval for publication.

Data availability of data

The datasets analysed during the current study are available from the corresponding author on reasonable request.

References

1. Allen CD, Breshears DD, McDowell NG (2015) On underestimation of global vulnerability to tree mortality and forest die-off from hotter drought in the Anthropocene. Ecosphere 6(8)
2. Allen CD, Macalady AK, Chenchouni H et al (2010) A global overview of drought and heat-induced tree mortality reveals emerging climate change risks for forests. Forest Ecology and Management 259(4):660–684
3. Anderson RG, Canadell JG, Randerson JT et al (2011) Biophysical considerations in forestry for climate protection. Frontiers in Ecology and the Environment 9(3):174–182
4. Archambeau J, Ruiz-Benito P, Ratcliffe S et al (2019) Similar patterns of background mortality across Europe are mostly driven by drought in European beech and a combination of drought and

competition in Scots pine. bioRxiv:551820

5. Aubin I, Boisvert-Marsh L, Kebli H et al (2018) Tree vulnerability to climate change: improving exposure-based assessments using traits as indicators of sensitivity. Ecosphere 9(2)
6. Baier P, Pennerstorfer J, Schopf A (2007) PHENIPS - A comprehensive phenology model of Ips typographus (L.) (Col., Scolytinae) as a tool for hazard rating of bark beetle infestation. Forest Ecology and Management 249(3):171–186
7. Bonneau M (1985) Le «nouveau dépérissement» des forêts. Symptômes, causes possibles, importance éventuelle de la nature des sols. Revue Forestière Française XXXVI(4): 239–251
8. Brandl S, Paul C, Knoke T, Falk W (2020) The influence of climate and management on survival probability for Germany's most important tree species. Forest Ecology and Management 458
9. Brockerhoff EG, Barbaro L, Castagneyrol B et al (2017) Forest biodiversity, ecosystem functioning and the provision of ecosystem services. Biodiversity and Conservation 26(13):3005–3035
10. Buras A, Rammig A, Zang CS (2020) Quantifying impacts of the 2018 drought on European ecosystems in comparison to 2003. Biogeosciences 17(6):1655–1672
11. Carnicer J, Coll M, Ninyerola M, Pons X, Sanchez G, Penuelas J (2011) Widespread crown condition decline, food web disruption, and amplified tree mortality with increased climate change-type drought. Proceedings of the National Academy of Sciences of the United States of America 108(4):1474–1478
12. Cavazzi S, Corstanje R, Mayr T, Hannam J, Fealy R (2013) Are fine resolution digital elevation models always the best choice in digital soil mapping? Geoderma 195:111–121
13. Charru M, Seynave I, Morneau F, Rivoire M, Bontemps J-D (2012) Significant differences and curvilinearity in the self-thinning relationships of 11 temperate tree species assessed from forest inventory data. Annals of Forest Science 69(2):195–205
14. Chen J, Franklin JF, Spies TA (1995) Growing-Season Microclimatic Gradients from Clearcut Edges into Old-Growth Douglas-Fir Forests. Ecological Applications 5(1):74–86
15. Choat B, Jansen S, Brodribb TJ et al (2012) Global convergence in the vulnerability of forests to drought. Nature 491(7426):752–756
16. Coops NC, Waring RH (2011) Estimating the vulnerability of fifteen tree species under changing climate in Northwest North America. Ecological Modelling 222(13):2119–2129
17. Das AJ, Slaton MR, Mallory J, Asner GP, Martin RE, Hardwick P (2022) Empirically validated drought vulnerability mapping in the mixed conifer forests of the Sierra Nevada. Ecological Applications 32(2)
18. Das AJ, Stephenson NL, Flint A, Das T, van Mantgem PJ (2013) Climatic Correlates of Tree Mortality in Water- and Energy-Limited Forests. Plos One 8(7)
19. de Groot M, Ogris N (2019) Short-term forecasting of bark beetle outbreaks on two economically important conifer tree species. Forest Ecology and Management 450

20. Dietze MC, Moorcroft PR (2011) Tree mortality in the eastern and central United States: patterns and drivers. Global Change Biology 17(11):3312–3326
21. Elling W, Dittmar C, Pfaffelmoser K, Rotzer T (2009) Dendroecological assessment of the complex causes of decline and recovery of the growth of silver fir (Abies alba Mill.) in Southern Germany. Forest Ecology and Management 257(4):1175–1187
22. Fielding AH, Bell JF (1997) A review of methods for the assessment of prediction errors in conservation presence/absence models. Environmental Conservation 24(1):38–49
23. Fremout T, Thomas E, Gaisberger H et al (2020) Mapping tree species vulnerability to multiple threats as a guide to restoration and conservation of tropical dry forests. Global Change Biology 26(6):3552–3568
24. Fujita S, Noguchi K, Tange T (2021) Different Waterlogging Depths Affect Spatial Distribution of Fine Root Growth for Pinus thunbergii Seedlings. Frontiers in Plant Science 12
25. Gazol A, Camarero J, Anderegg W, Vicente-Serrano S (2017) Impacts of droughts on the growth resilience of Northern Hemisphere forests. Global Ecology and Biogeography 26(2):166–176
26. Gazol A, Camarero JJ (2016) Functional diversity enhances silver fir growth resilience to an extreme drought. Journal of Ecology 104(4):1063–1075
27. Gegout JC, Hervé JC, Houllier F, Pierrat JC (1998) Using vegetation to predict PH in the Vosges mountains Forests. pp. 17
28. Gegout JC, Hervé JC, Houllier F, Pierrat JC (2003) Prediction of forest soil nutrient status using vegetation. Journal of Vegetation Science 14(1):55–62
29. Guinier P (1959) Trois conifères de la flore vosgienne. Bulletin de la société botanique de France 106(85):168–183
30. Han J, Singh VP (2020) Forecasting of droughts and tree mortality under global warming: a review of causative mechanisms and modeling methods. Journal of Water and Climate Change 11(3):600–632
31. Hartmann H, Moura CF, Anderegg WRL et al (2018) Research frontiers for improving our understanding of drought-induced tree and forest mortality. New Phytologist 218(1):15–28
32. Jaime L, Batllori E, Margalef-Marrase J, Pérez Navarro MÁ, Lloret F (2019) Scots pine (Pinus sylvestris L.) mortality is explained by the climatic suitability of both host tree and bark beetle populations. Forest Ecology and Management 448:119–129
33. King G, Zeng L (2001) Logistic Regression in Rare Events Data. Political Analysis 9:137–163
34. Knight KS, Brown JP, Long RP (2013) Factors affecting the survival of ash (Fraxinus spp.) trees infested by emerald ash borer (Agrilus planipennis). Biological Invasions 15(2):371–383
35. Kolb T, Keefover-Ring K, Burr SJ, Hofstetter R, Gaylord M, Raffa KF (2019) Drought-Mediated Changes in Tree Physiological Processes Weaken Tree Defenses to Bark Beetle Attack. Journal of Chemical Ecology 45(10):888–900

36. Landmann G, Bonneau M, Adrian M (1987) Le dépérissement du Sapin pectiné et de l'Epicéa commun dans le massif vosgien est-il en relation avec l'état nutritionnel des peuplements ? Revue forestière Française XXXIX (1):5–11
37. Lebourgeois F (2007) Climatic signal in annual growth variation of Silver Fir (Abies alba Mill.) and Spruce (Picea abies Karst) from the French Permanent Plot Network (RENECOFOR). Annals of Forest Science, 64 (3):333–343
38. Lebourgeois F, Gomez N, Pinto P, Mérian P (2013) Mixed stands reduce Abies alba tree-ring sensitivity to summer drought in the Vosges mountains, western Europe. Forest Ecology and Management 303:61–71
39. Lehmann A, Overton JM, Leathwick JR (2002) GRASP: generalized regression analysis and spatial prediction. Ecological Modelling 157(2–3):189–207
40. Lu LL, Wang HC, Chhin S, Duan AG, Zhang JG, Zhang XQ (2019) A Bayesian Model Averaging approach for modelling tree mortality in relation to site, competition and climatic factors for Chinese fir plantations. Forest Ecology and Management 440:169–177
41. Lundquist JE (2019) Impacts of Bark Beetles on Ecosystem Values in Western Forests-Introduction. Journal of Forestry 117(2):136–137
42. Manel S, Williams HC, Ormerod SJ (2001) Evaluating presence-absence models in ecology: the need to account for prevalence. Journal of Applied Ecology 38(5):921–931
43. Manion PD (1981) Tree disease concepts. Prentice-Hall
44. Maringer J, Stelzer AS, Paul C, Albrecht AT (2021) Ninety-five years of observed disturbance-based tree mortality modeled with climate-sensitive accelerated failure time models. European Journal of Forest Research 140(1):255–272
45. Marini L, Økland B, Jönsson AM et al (2017) Climate drivers of bark beetle outbreak dynamics in Norway spruce forests. Ecography 40(12):1426–1435
46. Mc Cook LJ (1994) Understanding ecological community succession: Causal models and theories, a review. Vegetatio 110:115–147
47. McCarthy JJ, Canziani OF, Leary NA, Dokken DJ, White KS (2001) Climate Change 2001: Impacts, Adaptation, and Vulnerability
48. McCullagh P, Nelder JA (1997) Generalized linear models. Chapman & Hall, London, UK
49. McDowell N, Pockman WT, Allen CD et al (2008) Mechanisms of plant survival and mortality during drought: why do some plants survive while others succumb to drought? New Phytologist 178(4):719–739
50. Mesquita RCG, Delamonica P, Laurance WF (1999) Effect of surrounding vegetation on edge-related tree mortality in Amazonian forest fragments. Biological Conservation 91(2–3):129–134
51. Michel A, Seidling W (2018) Forest Condition in Europe: 2018 Technical Report of ICP Forests. Report under the UNECE Convention on Long-Range Transboundary Air Pollution (CLRTAP). BFW Austrian Research Centre for Forests, Vienna, pp. 128

52. Neumann M, Mues V, Moreno A, Hasenauer H, Seidl R (2017) Climate variability drives recent tree mortality in Europe. Global Change Biology 23(11):4788–4797
53. Ols C, Bontemps JD (2021) Pure and even-aged forestry of fast-growing conifers under climate change: on the need for a silvicultural paradigm shift. Environmental Research Letters 16(2):5
54. Ondo I, Burns J, Piedallu C (2017) Including the lateral redistribution of soil moisture in a supra regional water balance model to better identify suitable areas for tree species. Catena 153:207–218
55. Pedersen BS (1998) Modeling tree mortality in response to short- and long-term environmental stresses. Ecological Modelling 105(2–3):347–351
56. Peng CH, Ma ZH, Lei XD et al (2011) A drought-induced pervasive increase in tree mortality across Canada's boreal forests. Nature Climate Change 1(9):467–471
57. Pfeifer EM, Hicke JA, Meddens AJ (2011) Observations and modeling of aboveground tree carbon stocks and fluxes following a bark beetle outbreak in the western United States. Global Change Biology 17(1):339–350
58. Piedallu C, Gégout J-C, Perez V, Lebourgeois F (2013) Soil water balance performs better than climatic water variables in tree species distribution modelling: Soil water balance improves tree species distribution models. Global Ecology and Biogeography 22(4):470–482
59. Piedallu C, Gegout JC (2007) Multiscale computation of solar radiation for predictive vegetation modelling. Annals of Forest Science 64(8):899–909
60. Piedallu C, Gegout JC, Bruand A, Seynave I (2011) Mapping soil water holding capacity over large areas to predict potential production of forest stands. Geoderma 160(3–4):355–366
61. Piedallu C, Gegout JC, Lebourgeois F, Seynave I (2016) Soil aeration, water deficit, nitrogen availability, acidity and temperature all contribute to shaping tree species distribution in temperate forests. Journal of Vegetation Science 27(2):387–399
62. Pörtner H-O, Roberts DC, Tignor M et al (2022) IPCC, 2022: Climate Change 2022: Impacts, Adaptation, and Vulnerability. Contribution of Working Group II to the Sixth Assessment Report of the Intergovernmental Panel on Climate Change. (eds.). Cambridge University Press. In Press.,
63. Preisler HK, Grulke NE, Heath Z, Smith SL (2017) Analysis and out-year forecast of beetle, borer, and drought-induced tree mortality in California. Forest Ecology and Management 399:166–178
64. Pretzsch H (2005) Stand density and growth of Norway spruce (Picea abies (L.) Karst.) and European beech (Fagus sylvatica L.): evidence from long-term experimental plots. European Journal of Forest Research 124(3):193–205
65. Pretzsch H, Grams T, Haberle KH, Pritsch K, Bauerle T, Rotzer T (2020) Growth and mortality of Norway spruce and European beech in monospecific and mixed-species stands under natural episodic and experimentally extended drought. Results of the KROOF throughfall exclusion experiment. Trees-Structure and Function 34(4):957–970
66. Pukkala T, Lähde E, Laiho O (2013) Species Interactions in the Dynamics of Even- and Uneven-Aged Boreal Forests. Journal of Sustainable Forestry 32(4):371–403

67. Rogers Brendan M, Solvik K, Hogg EH et al (2018) Detecting early warning signals of tree mortality in boreal North America using multiscale satellite data. Global Change Biology 24(6):2284–2304
68. Rotzer T, Haberle KH, Kallenbach C, Matyssek R, Schutze G, Pretzsch H (2017) Tree species and size drive water consumption of beech/spruce forests - a simulation study highlighting growth under water limitation. Plant and Soil 418(1–2):337–356
69. Roulleau (1912) Bulletin trimestriel de l'office forestier du centre et de l'Ouest tome 3(1ere série)
70. Rouse WR, Wilson RG (1969) Time and Space Variations in the Radiant Energy Fluxes Over Sloping Forested Terrain and Their Influence on Seasonal Heat and Water Balances at a Middle Latitude Site. Geografiska Annaler: Series A, Physical Geography 51(3):160–175
71. Schelhaas MJ, Nabuurs GJ, Schuck A (2003) Natural disturbances in the European forests in the 19th and 20th centuries. Global Change Biology 9(11):1620–1633
72. Senf C, Buras A, Zang CS, Rammig A, Seidl R (2020) Excess forest mortality is consistently linked to drought across Europe. Nature Communications 11(1)
73. Senf C, Pflugmacher D, Zhiqiang Y et al (2018) Canopy mortality has doubled in Europe's temperate forests over the last three decades. Nat Commun 9(1):4978
74. Sinclair WA (1965) Comparisons of recent declines of white ash, oaks, and sugar maple in northeastern woodlands. Cornell Plant 20:62–67
75. Staupendahl K, Zucchini W (2011) Estimating survival functions for the main tree species based on time series data from the forest condition survey in Rheinland-Pfalz, Germany. Allgemeine Forst Und Jagdzeitung 182(7–8):129–145
76. Suarez ML, Ghermandi L, Kitzberger T (2004) Factors predisposing episodic drought-induced tree mortality in Nothofagus - site, climatic sensitivity and growth trends. Journal of Ecology 92(6):954–966
77. Sun JB, Yang JY, Zhang C, Yun WJ, Qu JQ (2013) Automatic remotely sensed image classification in a grid environment based on the maximum likelihood method. Mathematical and Computer Modelling 58(3–4):573–581
78. Taccoen A, Piedallu C, Seynave I et al (2019) Background mortality drivers of European tree species: climate change matters. Proceedings of the Royal Society B-Biological Sciences 286(1900)
79. Thomas AL, Gegout JC, Landmann G, Dambrine E, King D (2002) Relation between ecological conditions and fir decline in a sandstone region of the vosges mountains (northeastern France). Annals of Forest Science 29:265–273
80. Thornthwaite CW, Mather JR (1955) The water balance. Laboratory of Climatology, Publication in Climatology. n°8
81. Torssonen P, Strandman H, Kellomaki S et al (2015) Do we need to adapt the choice of main boreal tree species in forest regeneration under the projected climate change? Forestry 88(5):564–572
82. Turc L (1961) Estimation of irrigation water requirements, potential evapotranspiration: a simple climatic formula evolved up to date. Ann Agron 12(1):13–49

83. Urli M, Porté AJ, Cochard H, Guengant Y, Burlett R, Delzon S (2013) Xylem embolism threshold for catastrophic hydraulic failure in angiosperm trees. Tree Physiology 33(7):672–683
84. van Mantgem PJ, Stephenson NL, Byrne JC et al (2009) Widespread Increase of Tree Mortality Rates in the Western United States. Science 323(5913):521–524
85. Verbesselt J, Robinson A, Stone C, Culvenor D (2009) Forecasting tree mortality using change metrics derived from MODIS satellite data. Forest Ecology and Management 258(7):1166–1173
86. Vitali V, Buntgen U, Bauhus J (2017) Silver fir and Douglas fir are more tolerant to extreme droughts than Norway spruce in south-western Germany. Global Change Biology 23(12):5108–5119
87. Ward NL, Masters GJ (2007) Linking climate change and species invasion: an illustration using insect herbivores. Global Change Biology 13(8):1605–1615
88. Western AW, Zhou S-L, Grayson RB, McMahon TA, Blöschl G, Wilson DJ (2004) Spatial correlation of soil moisture in small catchments and its relationship to dominant spatial hydrological processes. Journal of Hydrology 286(1):113–134
89. Williams AP, Allen CD, Macalady AK et al (2013) Temperature as a potent driver of regional forest drought stress and tree mortality. Nature Climate Change 3(3):292–297

Table

*Table 1: List of the 113 explanatory variables. All climate data were averaged over the 2009-2019 period, climate anomalies were differences between the 2009-2019 and 1961-1985 periods, and climate trends were the coefficients of regression calculated over the 1986-2019 period. wi = winter, sp = spring, su = summer, au = autumn, an = annual values. * monotonic and quadratic responses were evaluated, ** qualitative variables.*

	Category	Variable	Description	Source
STAND DESCRIPTION	STAND	COMP **	Stand composition: 4 levels of mixture	2018 aerial photographs
		DENS **	Stand density	
		STRUCT **	Stand structure	
		TYP_EDGE **	Presence of edges in the plot	
		EDGE_S **	Presence of an edge southward	
		STORM **	Forest damaged by the 1999 storm	IGN
SITE CONDITIONS	GEOLOGY	GEOL**	Simplified geological map	BRGM
	TOPOGRAPHY	ALT *	Altitude (m)	50 m resolution digital elevation model (DEM)
		COS_ASP *	Cosine of aspect	
		SIN_ASP *	Sine of aspect	
		SLO*	Slope (°)	
		CONT*	Containment in a 1,500-m radius (m.)	
		CURV*	Shape of the topographical surface (1,500-m radius)	
		TOPO*	Relative distance between ridge and talweg (m.)	
		REL_ALT*	Relative altitude between ridge and talweg (m.)	
		CURV*	Shape of the topographical surface (1,500-m radius)	
	SOIL NUTRITION	PH*	Bioindicated soil surface pH	(Gegout et al. 2003)
		CN*	Bioindicated soil surface C/N	
	SOIL WATER-LOGGING	TW*	Bioindicated temporary waterlogging	

		PW*	Bioindicated permanent waterlogging	
	ENERGY	RAD (wi, sp, su, an)	Solar radiation (2009-2019 period, J/cm²)	(Piedallu and Gegout 2007)
		TMIN_(wi, sp)	Minimum temperature (2009-2019 period, °C)	(Piedallu et al. 2016)
		TMEAN (wi, sp, su, au, an)	Mean temperature (2009-2019 period, °C)	
		TMAX (su)	Maximum temperature (2009-2019 period, °C)	
	CLIMATIC WATER CONTENT	RAIN (wi, sp, su, au, an)	Cumulated rainfall (2009-2019 period, mm)	
		CWB (wi, sp, su, au, an)	Climatic water balance (2009-2019 period)	
	SOIL WATER CONTENT	DEPTH	Soil depth	(Piedallu et al. 2011)
		SWHC	Soil water holding capacity (mm)	
		SWC (sp, su, au, an)	Soil water content (Thornthwaite formula, 2009-2019 period)	(Piedallu et al. 2013; Thornthwaite and Mather 1955)
		SWD (sp, su, au, an)	Soil water deficit (PET-AET, 2009-2019 period)	
	SOIL WATER FLUXES	Kh	Horizontal hydraulic conductivity at saturation (m *per* day)	(Ondo et al. 2017)
		Kv	Vertical hydraulic conductivity (m *per* day)	
		FLUX (su, an)	Lateral surface and subsurface fluxes (mm)	
CLIMATE EVOLUTION	CLIMATE ANOMALIES	evTMIN (wi, sp)	Evolution of minimum temperature (°C)	
		evTMEAN	Evolution of mean temperature (°C)	

	(wi, sp, su, au, an)	
	evTMAX (su)	Evolution of maximum temperature (°C)
	evRAIN (wi, sp, su, au, an)	Evolution of rainfall (mm)
	evCWB (wi, sp, su, au, an)	Evolution of CWB (mm)
	evSWC (wi, sp, su, au, an)	Evolution of SWC (mm)
	evSWD (wi, sp, su, au, an)	Evolution of SWD (mm)
CLIMATE TRENDS	regTMIN (wi, sp)	Minimum temperature trend
	regTMEAN (wi, sp, su, au, an)	Mean temperature trend
	regTMAX (su)	Maximum temperature trend
	regRAIN (wi, sp, su, au, an)	Rainfall trend
	regCWB (wi, sp, su, au, an)	CWB trend
	regSWC (wi, sp, su, au, an)	SWC trend
	regSWD (wi, sp, su, au, an)	SWD trend

Figures

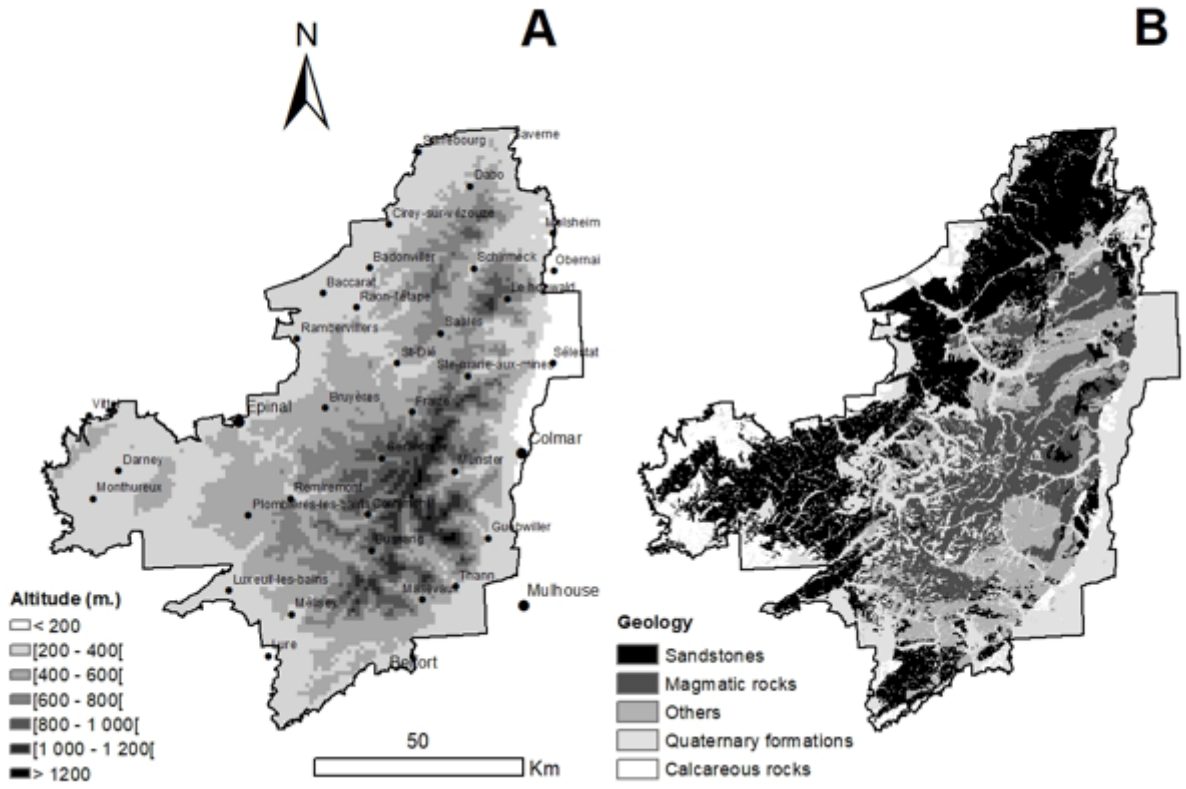

Figure 1

Localisation of the study area, distribution of altitudes (A) and simplified geological map (B).

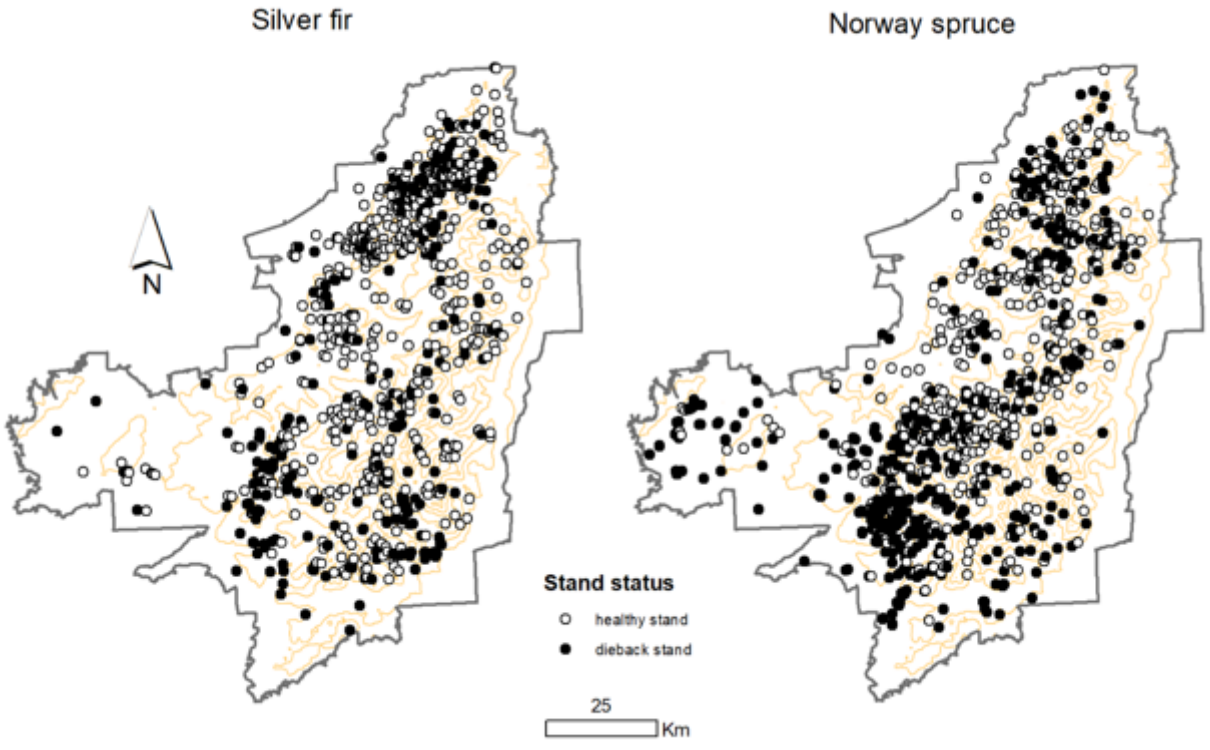

Figure 2

Localisation of the stands with dieback symptoms for silver fir (n= 872) and Norway spruce (n= 1,043) in the Vosges mountains.

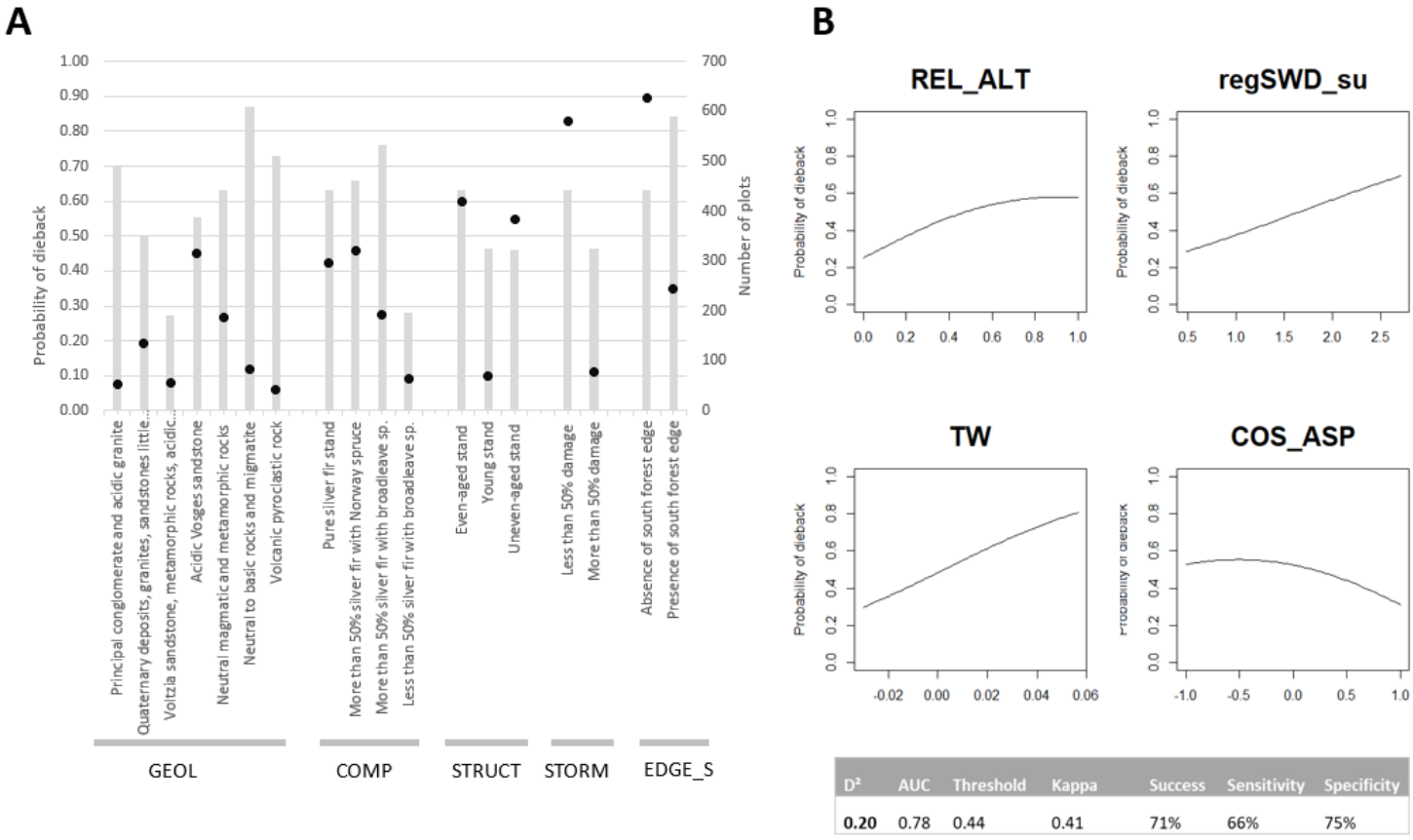

D²	AUC	Threshold	Kappa	Success	Sensitivity	Specificity
0.20	0.78	0.44	0.41	71%	66%	75%

Figure 3

Performances of the silver fir model and differences in the probability of dieback according to the variables (A: qualitative variables, B: quantitative variables). The response curves were calculated using mean values for the other quantitative variables, and the following modalities for the qualitative variables: GEOL, "Neutral magmatic and metamorphic rocks", EDGE_S, "Absence of a south forest edge", STRUCT, "Even-aged stand", COMP: "Pure silver fir stand", and STORM: "Less than 50% damage during the 1999 storm". Black dots in fig. 3A: numbers of plots for each modality.

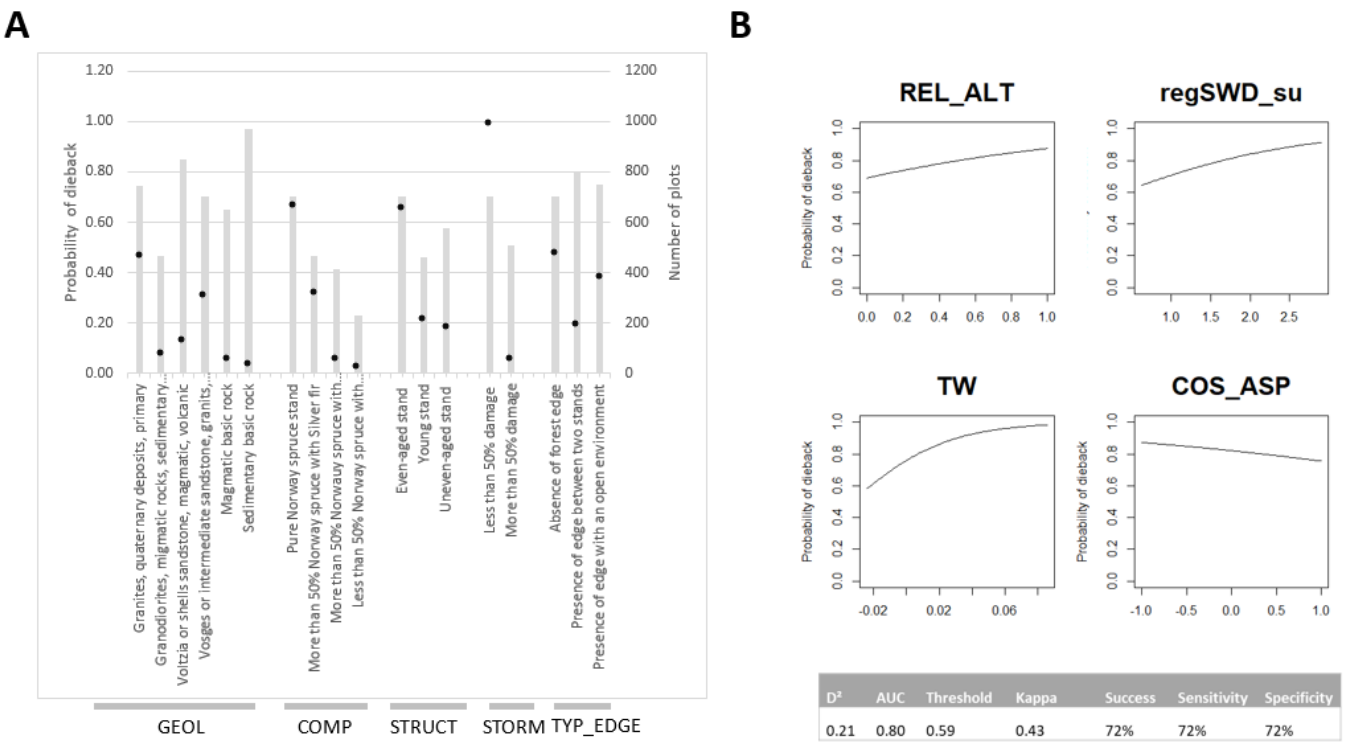

Figure 4

Performances of the Norway spruce model and differences in the probability of dieback according to the variables (A: qualitative variables, B: quantitative variables). The response curves were calculated using mean values for the other quantitative variables, and the following modalities for the qualitative variables: GEOL, "Vosges or intermediate sandstone, granites, gneiss", COMP_SAP: "pure Norway spruce stand", STRUCT, "even-aged stand", STORM, "Less than 10% damage during the 1999 storm", and TYP_EDGE "Absence of a forest edge". Black dots in fig. 4A: numbers of plots for each modality.

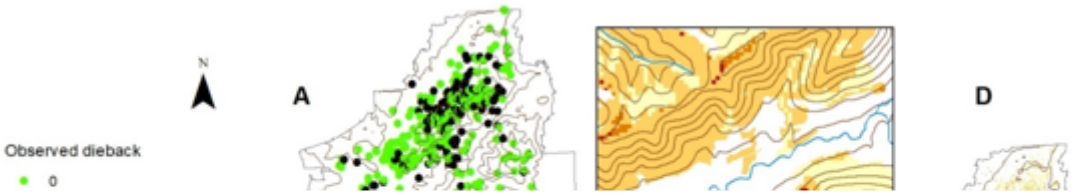

Figure 5

Silver fir dieback observed (A) or predicted in the sampled plots (B, C, n = 872), and vulnerability map (D). B: Dieback explained by environmental conditions only (variables GEOL, REL_ALT, regSWD_su, TW and COS_ASP). C: modulation of vulnerability predicted on map B due to the stand characteristics (variables COMP, STRUCT, EDGE_S and STORM). D: The vulnerability map was calculated with the modalities "Absence of a south forest edge", "Even-aged stand", "Pure silver fir stand" for the variables EDGE_S, STRUCT and COMP, respectively). The "high level of risk" class corresponds to the values greater than the optimal threshold obtained from the ROC curve; lower values were divided in three classes of equal interval (the break values are used for the legend on map B).

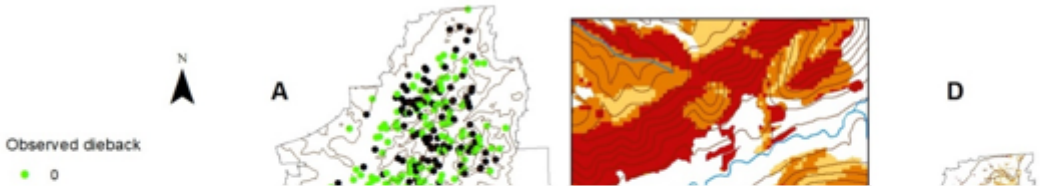

Figure 6

Norway spruce dieback observed (A) or predicted in the sampled plots (B, C, n = 1,043), and vulnerability map (D). B: Dieback explained by environmental conditions (variables GEOL, REL_ALT, regSWD_su, TW and COS_ASP). C: modulation of vulnerability predicted on map B due to the stand characteristics (variables COMP, STRUCT, STORM and TYP_EDGE). D: The vulnerability map was calculated with the modalities "pure Norway spruce stand", "even-aged stand", and "absence of a forest edge" for the variables COMP, STRUCT and TYP_EDGE, respectively. The "high level of risk" class corresponds to the values greater than the optimal threshold from the ROC curve; lower values are divided in three classes of equal interval (the break values are used for the legend on map B).

Figure 7

Distribution of the surfaces (%) with the different levels of risk for the silver fir and Norway spruce stands.

Figure 8

Volume of dead trees (m^3/ha) recorded in the silver fir and Norway spruce stands (ONF), according to the four levels of risk (trees inventoried in 2019 or between 2018 and 2020).

Supplementary Files

This is a list of supplementary files associated with this preprint. Click to download.

- Supplementarymaterial.docx